Supplemental Material to the article
"Cubic symmetry breaking in rare-earth dodecaborides with dynamic charge stripes"

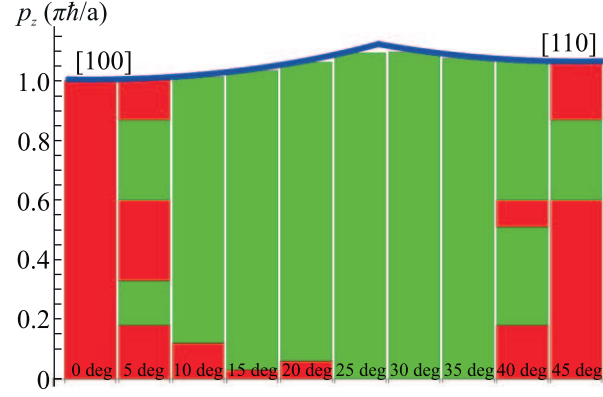Fig. S1. Distribution of the momentum projection p_z, at which open (green) and closed (red) trajectories are realized for different **H** directions. The rotation was performed around the [001] direction with a step of 5 degrees. The blue line shows the Brillouin zone boundary

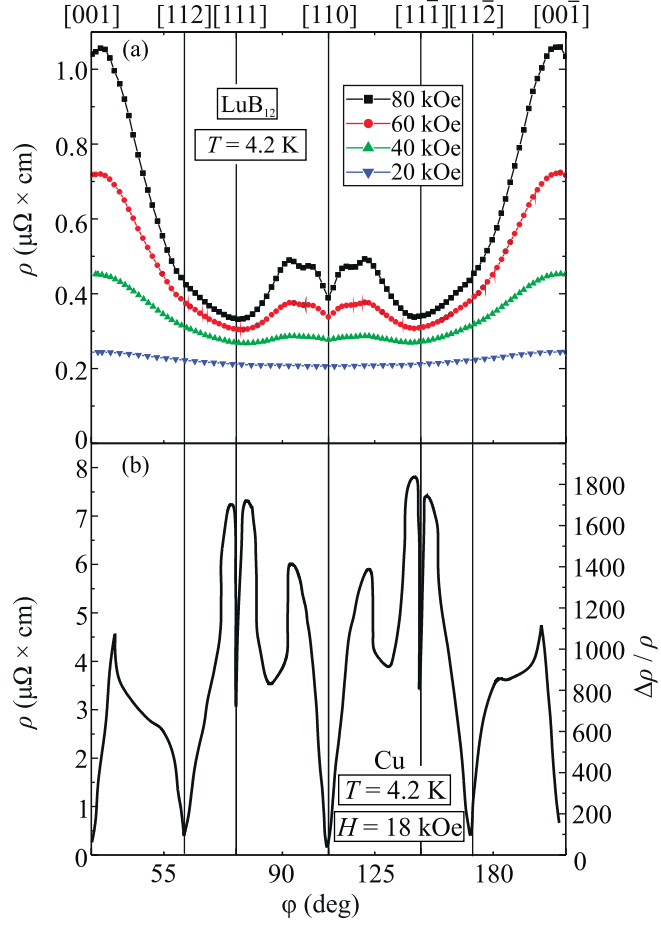Fig. S2. Angular dependences of the resistivity of LuB_{12} (a) and Cu (b) at temperature $T = 4.2$ K. The rotation was performed around the direction $\mathbf{I} \| [1\bar{1}0]$. The vertical lines show the principal directions in the fcc lattice

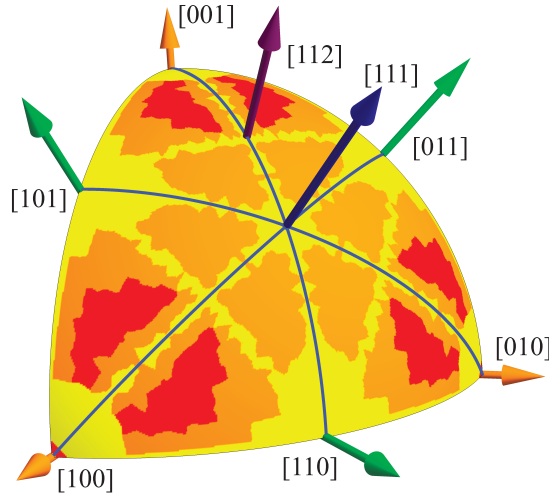Fig. S3. Schematic view of the possible magnetic field **H** directions leading to open trajectories (yellow areas), closed trajectories (red areas), and trajectories that are closed, but extending to 10 or more Brillouin zones in reciprocal space (orange areas) for the FS of copper. The arrows indicate the principal directions in the fcc lattice
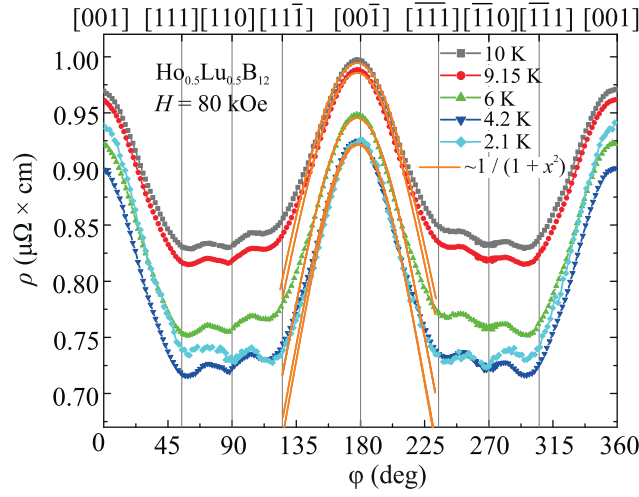

Fig. S4. Angular dependences of the $Ho_{0.5}Lu_{0.5}B_{12}$ resistivity in the external magnetic field $H = 80\,kOe$ in the temperature range 2.1–10 K. Solid orange lines show the approximation by $\rho = \rho_0/(1 + B(\varphi - \varphi_0)^2$
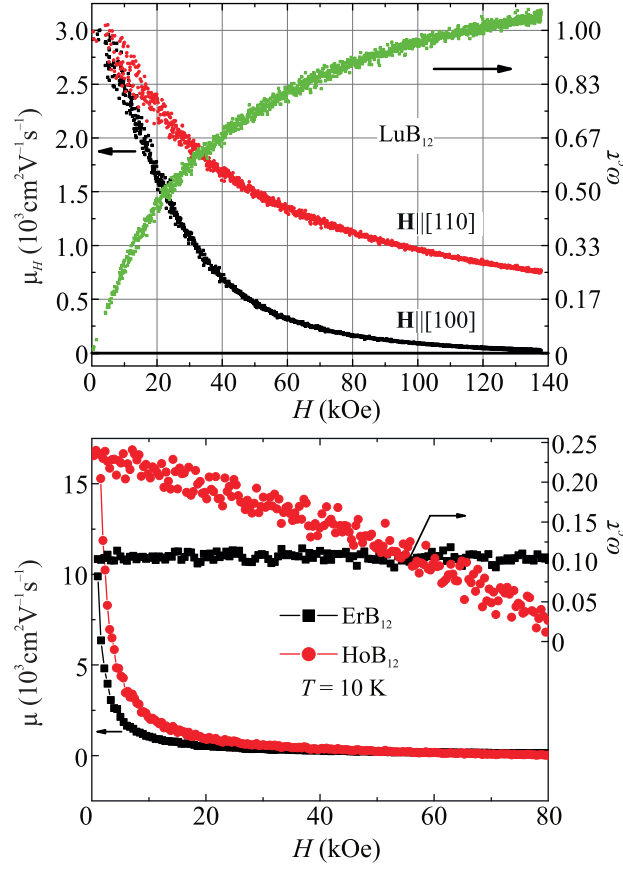
Fig. 5. Field dependences of the mobility (left axis) and the product of the cyclotron frequency ω_c by the average relaxation time τ (right axis) for LuB_{12} at $T = 4.2\,K$ (upper panel) and for ErB_{12} and HoB_{12} at $T = 10\,K$ (lower panel)
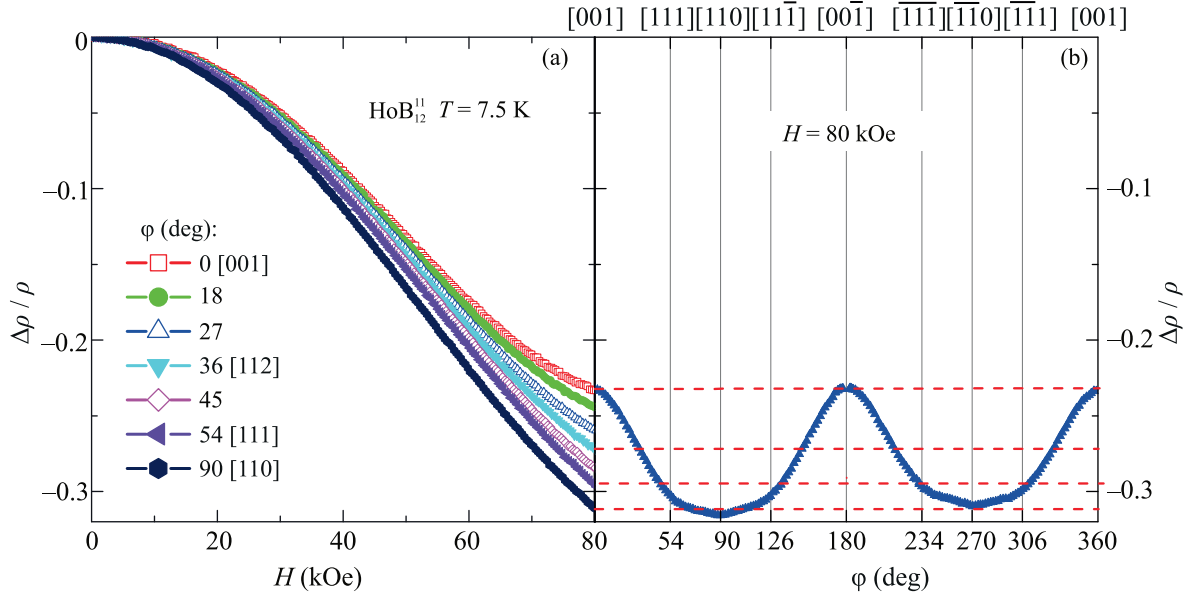

Fig. 6. Magnetic field (a) and angular (b) dependences of the magnetoresistance in the paramagnetic phase of HoB_{12} at $T = 7.5\,K$